Paramagnetic Ionic Liquid 1-Butyl-3-methylimidazolium Tetrabromidocobaltate(II): Activity Coefficients at Infinite Dilution of Organic Solutes and Crystal Structure†

Svetlana A. Kozlova, Sergey P. Verevkin, and Andreas Heintz*

Department of Physical Chemistry, University of Rostock, Hermannstr. 14, D-18051 Rostock, Germany

Tim Peppel and Martin Köckerling*

Department of Inorganic Chemistry, University of Rostock, Albert-Einstein-Str. 3a, D-18059 Rostock, Germany

Activity coefficients at infinite dilution, γ_i^∞, of different solutes (alkanes, alkenes, and alkylbenzenes as well as of the linear C_1-C_6 alcohols) in the paramagnetic ionic liquid 1-butyl-3-methylimidazolium tetrabromidocobaltate(II), $(C_4MIm)_2[CoBr_4]$, have been determined by gas chromatography using the ionic liquid as the stationary phase. The measurements were carried out at different temperatures between (308 and 413) K. From the temperature dependence of the limiting activity coefficients, partial molar excess enthalpies at infinite dilution $H_i^{E,\infty}$ of the solutes in the ionic liquid have been derived. Values of γ_i^∞ of solutes in the paramagnetic ionic liquid $(C_4MIm)_2[CoBr_4]$ have been compared at 298 K with results of γ_i^∞ for ionic liquids containing the 1-butyl-3-methylimidazolium cation and different nonmagnetic anions. No significant effects caused by the paramagnetic anion have been observed. Furthermore, the single-crystal X-ray structure has been determined. It crystallizes monoclinic (*C*2/c), $a = 16.7027(7)$, $b = 10.3163(4)$, $c = 15.4136(7)$ Å, and $\beta = 114.246(2)°$. The structure consists of isolated tetrahedral $[CoBr_4]^{2-}$ complex anions and 1-butyl-3-methylimidazolium cations.

1. Introduction

Imidazolium-based ILs with magnetic properties have attracted much interest recently.[1−4] It turned out that such ILs containing $[FeCl_4]^-$ or $[CoBr_4]^-$ as anions are paramagnetic liquids which show a distinct response to inhomogeneous magnetic fields.[4] In contrast to ferromagnetic fluids which consist of magnetic nanoparticles dispersed in a suitable solvent, magnetic ILs are real molecular dispersed fluids. They are paramagnetic even at lower temperatures since the repulsive negative Coulomb forces acting between the anions prevent the magnetic anions from building up effective magnetic interactions leading to ferromagnetism. Such paramagnetic ILs could be interesting for new technological applications. The first physicochemical measurements of mixtures containing the magnetic ionic liquid $(C_4MIm)[FeCl_4]$ have been published recently.[5] In this work, we extend our measurements of activity coefficients in infinite dilution γ_i^∞ in paramagnetic ionic liquids (IL) to the compound 1-butyl-3-methylimidazolium tetrabromidocobaltate(II) ($C_{16}H_{30}N_4CoBr_4$) having the molar mass 380.51 g·mol^{-1} and the common abbreviation $(C_4MIm)_2[CoBr_4]$.

Since ionic liquids have a negligible vapor pressure,[5] the most suitable method for measuring limiting activity coefficients of volatile solutes in ionic liquids is the gas−liquid chromatographic method using the ionic liquid as the stationary phase. A series of hydrocarbons such as alkanes, alkenes, and alkylbenzenes as well as linear C_1-C_6 alcohols in the ionic liquid $(C_4MIm)_2[CoBr_4]$ have been studied in the temperature range (308 to 413) K. Furthermore, the results of a single-crystal X-ray structure determination of $(C_4MIm)_2[CoBr_4]$ are reported in this paper.

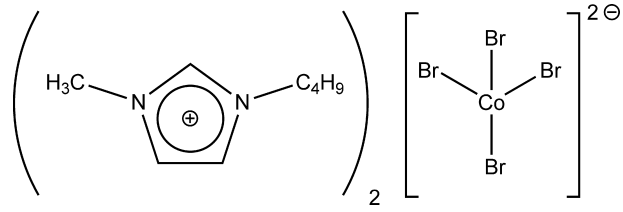

2. Experimental Section

2.1. Materials and Analytics. The samples of solutes studied were of commercial origin. GC analysis gave a purity of > 99.9 % in agreement with specifications stated by the suppliers. All chemicals were used without further purification. We used the following equipment: DSC, Mettler Toledo DSC823e (Rate 5 K·min^{-1}, Gas N2); IR, Nicolet Portégé 460; UV/V, Perkin-Elmer Lambda 2 (quartz cuvette: suprasil (R) $d = 10$ mm); NMR, Bruker AC 250 F; Elemental analysis, CE Instruments, Flash EA 1112 NC Analyzer.

2.2. Synthesis of $(C_4MIm)_2[CoBr_4]$. The synthesis of 1-butyl-3-methylimidazolium bromide $(C_4MIm)Br$ is well established and is described in the Supporting Information. Anhydrous $CoBr_2$ (1.1 g, 5.0 mmol) and 1-butyl-3-methylimidazolium bromide $(C_4MIm)Br$ (2.2 g, 10.0 mmol) are heated under reflux in 100 mL of dry acetonitrile until a clear deep blue solution is obtained. The solvent is evaporated, and the residue is washed thoroughly several times with small amounts of dry 2-propanol.

* To whom correspondence should be addressed. E-mail: andreas.heintz@uni-rostock.de.

† Part of the "Gerhard M. Schneider Festschrift".

10.1021/je800846j CCC: $40.75
Published on Web 03/03/2009

To crystallize the blue sticky residue, the following procedure is used: The residue is frozen in liquid nitrogen until it is completely solidified. This glassy solid is treated with a mixture of dry diethyl ether and 2-propanol (1:1) under slow warming up to 273 K until a blue powder is obtained. Finally, the solid is separated by filtration, washed several times with dry diethyl ether, and dried in vacuum. Yield: 3.1 g (93 %); mp = 318 K. CHN-analysis for $C_{16}H_{30}N_4CoBr_4$ [found (calculated)]: C 29.43 (29.25); H 4.59 (4.60); N 8.61 (8.53). IR (KBr, cm^{-1} ν_{max}): 3134, 3098, 3081, 2956, 2935, 2872, 1562, 1460, 1165, 842, 739, 624. UV/vis (λ_{max}/nm in acetone, RT): 619, 642, 668, 700, 723.

2.3. Measurements of the Activity Coefficients. Chromosorb W/AW-DMCS 100/120 mesh was used as solid support for the ionic liquid in the GC column. The chromosorb has been subjected to vacuum treatment with heating to remove traces of adsorbed moisture prior to use. Coating the solid support material with the ionic liquid was performed by dispersing the needed portion of chromosorb in a solution of the ionic liquid in dichloromethane followed by evaporation of the solvent using a rotating evaporator. The chromosorb was weighed before and after the coating process. The measurements of the activity coefficients were performed with a Hewlett-Packard gas chromatograph equipped with a flame ionization detector. Nitrogen was used as the carrier gas. A GC column (stainless steel) with a length of 45 cm and with an inside diameter of 0.40 cm was used. The amount of stationary phase (ionic liquid) was 1.3353 mmol. The mass of the stationary phase was determined with a precision of ± 0.0003 g. To avoid possible residual adsorption effects of the solutes on chromosorb, the amount of ionic liquid was 26.69 mass percent of the support material.

According to Cruickshank et al.,[6] the following equation for the data treatment was used

$$\ln \gamma_{i,3}^{\infty} = \ln\left(\frac{n_3 \cdot R \cdot T}{V_N \cdot p_1^0}\right) - \frac{B_{11} - V_1^0}{RT} \cdot p_1^0 + \frac{2 \cdot B_{12} - V_1^{\infty}}{RT} \cdot J \cdot p_0 \quad (1)$$

where $\gamma_{i,3}^{\infty}$ is the activity coefficient of component i at infinite dilution in the stationary phase (index 3); p_1^0 is the vapor pressure of the pure liquid solute; n_3 is the number of moles of the stationary phase component (ionic liquid) on the column; and V_N is the standardized retention volume obtained by

$$V_N = J \cdot U_0 \cdot (t_r - t_G) \cdot \frac{T_{col}}{T_f} \cdot \left[1 - \frac{p_{ow}}{p_o}\right] \quad (2)$$

where t_r is the retention time; t_G is the dead time; U_0 is the flow rate, measured by a soap bubble flowmeter; T_{col} is the column temperature; T_f is flowmeter temperature; p_{ow} is saturation vapor pressure of water at T_f; and p_o is the pressure at the column outlet.

The second and third term in eq 1 are correction terms which arise from the nonideality of the mobile gaseous phase. B_{11} is the second virial coefficient of the solute, and B_{12} is the mixed virial coefficient of the solute (1) with the carrier gas nitrogen (2). V_1^0 is the liquid molar volume of the pure solute, and V_1^{∞} is the partial molar volume of solute in the ionic liquid at infinite dilution.

The factor J appearing in eqs 1 and 2 corrects for the influence of the pressure drop along the column given by[7]

$$J = \frac{3}{2} \cdot \frac{(p_i/p_o)^2 - 1}{(p_i/p_o)^3 - 1} \quad (3)$$

where p_i and p_o are the inlet and the outlet pressure of the GC column, respectively.

The outlet pressure p_o was kept equal to the atmospheric pressure. The pressure drop ($p_i - p_o$) was varied between (20.3 and 101.3) kPa, providing suitable retention times with sharp peaks. The pressure drop and the outlet pressure were measured using a membrane manometer with an uncertainty of ± 0.2 kPa.

Volumes of the samples injected into the GC probes were (0.5 to 2) μL. No differences in retention times t_r were found by injecting individual pure components or their mixtures. This fact indicates that different concentrations of the solute in the stationary phase caused by different ratios of the injected amounts of solute and the amount of stationary phase do not affect the results. It can be concluded that in all cases the state of infinite dilution was realized to a high degree of approximation. Experiments were carried out at four to five temperatures (in 10 degree steps) between (308 and 413) K. The temperature of the GC column was maintained constant within ± 0.01 K. At a given temperature, each experiment was repeated at least twice to check the reproducibility. Retention times were generally reproducible within (0.01 to 0.03) min. Absolute values of retention times varied between (3 to 30) min depending on the individual solute. At each temperature, values of the dead time t_G identical to the retention time of a nonretainable component were measured. While our GC is equipped with a flame-ionization detector, methane was used as a nonretainable component under the assumption that the effect of solubility of methane in ionic liquid is negligible. This assumption has been justified by attestation of our experimental procedure with the reliable data on γ_i^{∞} of hexane, heptane, and benzene in hexadecane.

To check the stability of the experimental conditions, such as the possible elution of the stationary phase by the nitrogen stream, the measurements of retention times were repeated systematically every (2 to 3) days for three selected solutes. No changes of the retention times were observed during several months of continuous operation.

Data needed for calculating the correction terms in eq 1 are given in the Supporting Information. Values of vapor pressures p_1^0 of pure solutes are of crucial importance for the reliability of γ_i^{∞}. For alkanes these values were calculated using parameters of the Cox equation recommended by Ruzicka and Majer[8] and for alkenes those recommended by Steele and Chirico.[9] Vapor pressures of pure alcohols were calculated using coefficients of Wagner's equation recommended by Ambrose and Walton.[10] Specification of the sources of vapor pressures of other solutes was given in previous papers of this series.[11−15]

The validity of the experimental procedure has been checked by comparison of our measured values of γ_i^{∞} for hexane in hexadecane with those available in the literature.[11] The procedure of the experimental error estimation was described in our previous work.[11] Values of γ_i^{∞} are estimated to be accurate to within ± 3 %.

2.4. X-Ray Structure Determination. A suitable dark blue single crystal for X-ray diffraction experiments was obtained by cooling the liquid $(C_4MIm)_2[CoBr_4]$ quickly to 233 K and storing the material at that temperature for several days. This treatment avoided glassy solidification of this IL, and slow heating to 273 K gave suitable single crystals.

Table 1. Experimental Results of γ_i^∞ for Different Solutes in the $(C_4MIm)_2[CoBr_4]$: Temperature Ranges, Coefficients of Equation 4, γ_i^∞ at 298 K Calculated Using Equation 4, and Values of $H_i^{E,\infty}$ Derived from Equation 5

solute *i*	temperature interval / K	*a*	*b* / K	$\gamma_{i\,(298\ K)}^\infty$	$H_i^{E,\infty}$ / kJ·mol^{-1}
		alkanes			
octane	308 to 333	0.924	881.74	48.49	7.33
nonane	308 to 343	0.784	1006.7	64.10	8.37
decane	308 to 353	0.589	1145	83.9	9.52
undecane	333 to 373	−0.194	1495.6	124.3	12.44
dodecane	343 to 383	−0.699	1762.9	183.8	14.66
		alkenes			
1-octene	313 to 353	0.892	707.1	26.1	5.88
1-decene	313 to 353	1.417	739.54	27.3	6.15
		alkylbenzene			
benzene	308 to 323	3.19	−842.62	1.44	−7.0
toluene	308 to 333	0.043	302.34	2.88	2.51
ethyl benzene	323 to 373	0.308	400.99	5.22	3.33
propyl benzene	313 to 373	0.880	399.27	9.20	3.32
butyl benzene	313 to 373	1.217	438.57	14.7	3.65
pentyl benzene	333 to 373	1.633	452.92	23.4	3.77
		alcohols			
methanol	308−333	−2.295	568.99	0.68	4.73
ethanol	308−333	−2.897	864.29	1.00	7.19
1-propanol	323−373	−3.322	1162.1	1.78	9.66
1-butanol	333−393	−2.838	1095.3	2.31	9.11
1-pentanol	353−413	−2.684	1172.4	3.49	9.75
1-hexanol	353−393	−2.086	1096.7	4.91	9.12

Table 2. Comparison of Values of γ_i^∞ of Typical Solutes at 298 K in Butylimidazolium-Based ILs Derived in the Present Work and Those from the Literature

solute *i*	$(C_4MIm)_2[CoBr_4]$ this work	$[C_4MIm][FeCl_4]$ ref 5	$[C_4MIm][NTf_2]$ ref 14
decane	83.9	68.5	64.5
1-decene	27.3	27.3	34.4
toluene	2.88	1.03	1.40
methanol	0.68	1.85	1.30

A crystal of size 0.15 × 0.14 × 0.10 mm^3 was selected under a microscope and quickly fixed with grease on the tip of a thin glass rod and placed in the cold nitrogen stream (173 K) on the goniometer of a Bruker-Nonius Apex-X8 diffractometer, equipped with a CCD-detector. Graphite monochromated Mo Kα radiation ($\lambda = 0.71073$ Å) was used. First, unit cell dimensions were obtained from the reflections, which were taken from a total of 36 frames, measured in three different crystal directions. Data collection and reduction including corrections for Lorentz and polarization effects were done using Bruker-Nonius Inc. Software.[16] The structure was solved via Direct Methods and refined by full-matrix least-squares methods on F^2 using the SHELX-97 program package.[17] All atoms (except hydrogen) were treated

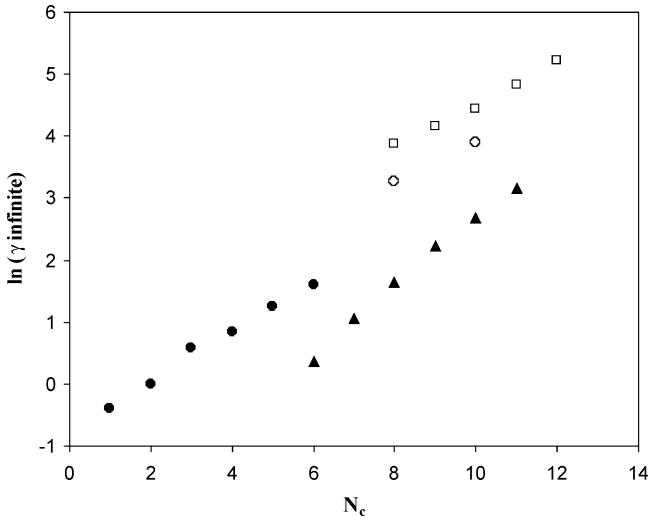

Figure 1. Values of ln(γ_i^∞) as a function of the number of carbon atoms N_C for different classes of solutes in $(C_4MIm)_2[CoBr_4]$ at 298 K: □, alkanes; ○, alkenes; ▲, alkylbenzenes; ●, alcohols.

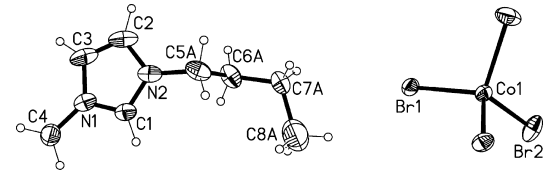

Figure 2. Ortep plot of $(C_4MIm)_2[CoBr_4]$ with atom numbering scheme (atomic displacement ellipsoids with 50 % probability). Only one of the two disordered butyl chains is shown.

Table 3. Crystal and Refinement Data for $(C_4MIm)_2[CoBr_4]$

empirical formula	$C_{16}\ H_{30}\ N_4\ Co\ Br_4$
formula weight (g·mol^{-1})	657.01
temperature	173(2) K
wavelength	0.71073 Å
crystal system	monoclinic
space group	*C*2/c (no. 15)
unit cell dimensions	
a	16.7027(7) Å
b	10.3163(4) Å
c	15.4136(7) Å
β	141.246(2)
volume, *Z*	2421.6(2) Å^3, 4
density (calculated)	1.802 g·cm^{-3}
absorption coefficient	7.32 mm^{-1}
crystal size	(0.15 × 0.14 × 0.10) mm^3
theta range for data collection	4.3 to 32.6°
reflections collected	15425
independent reflections	4330 [R(int) = 0.024]
absorption correction	semiempirical, based on equivalents (SADABS)[16]
refinement method	full-matrix least-squares on F^2
data/restraints/parameters	4330/0/134
goodness-of-fit on F^2	1.04
final R indices $[I > 2\sigma(I)]^{a,b}$	$R1 = 0.028$, $wR2 = 0.062$
R indices (all data)^{a,b}	$R1 = 0.047$, $wR2 = 0.065$
largest diff. peak and hole	(0.91 and −0.93) e·Å^{-3}

^{a} $R1 = (\sum ||F_o| - |F_c||)/(\sum |F_o|)$. ^{b} $wR2 = [(\sum w(|F_o^2| - |F_c^2|)^2)/(\sum w(F_o^2)^2)]^{1/2}$; for all data, with $w = 1/[(\sigma^2(F_o^2) + (0.0306P)^2 + 0.9811P]$; $P = (F_o^2 + 2F_c^2)/3$.

Table 4. Atomic Coordinates and Equivalent Isotropic Displacement Parameters (Å^2) in $(C_4MIm)_2[CoBr_4]^a$

atom	*x*	*y*	*z*	U_{eq}
Co1	0.5	0.22827(3)	0.25	0.02651(8)
Br1	0.38999(1)	0.09552(2)	0.13266(1)	0.03270(6)
Br2	0.57587(1)	0.35777(2)	0.17799(2)	0.04830(8)
N1	0.1313(1)	−0.7777(2)	0.0722(1)	0.0348(4)
C1	0.1958(1)	−0.6929(2)	0.1130(1)	0.0328(4)
N2	0.1630(1)	−0.5866(2)	0.1347(1)	0.0362(4)
C2	0.0744(2)	−0.6052(3)	0.1065(2)	0.0501(6)
C3	0.0549(1)	−0.7226(3)	0.0668(2)	0.0494(6)
C4	0.1404(2)	−0.9034(2)	0.0336(2)	0.0419(5)
C5A	0.2127(2)	−0.4683(2)	0.1761(2)	0.0430(5)
C6A	0.2134(3)	−0.3682(4)	0.0985(3)	0.040(1)
C7A	0.2790(4)	−0.2577(5)	0.1349(4)	0.043(1)
C8A	0.3777(2)	−0.2889(4)	0.1424(3)	0.103(1)
C5B	0.2127(2)	−0.4683(2)	0.1761(2)	0.0430(5)
C6B	0.2637(3)	−0.4333(4)	0.1258(3)	0.041(1)
C7B	0.3155(4)	−0.3106(6)	0.1689(5)	0.054(2)
C8B	0.3777(2)	−0.2889(4)	0.1424(3)	0.1023(1)

^{a} U_{eq} is defined as one third of the trace of the orthogonalized U^{ij} tensor.

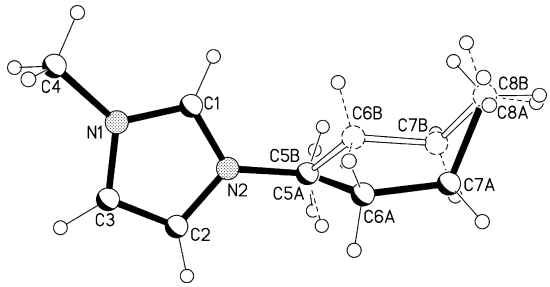

Figure 3. View of the cation of $(C_4MIm)_2[CoBr_4]$ showing the disorder of the butyl group.

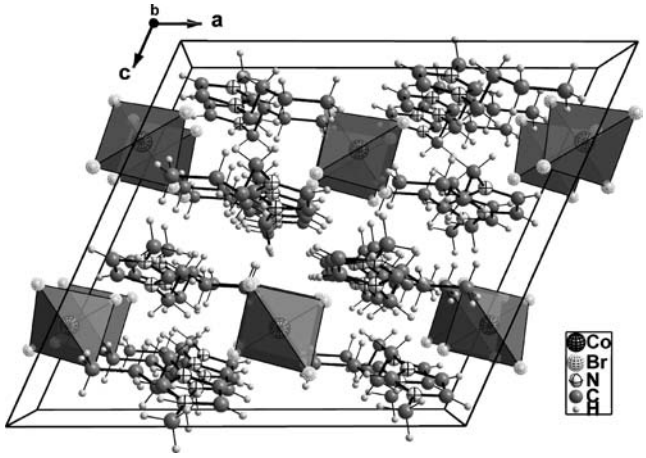

Figure 4. View of the contents of the unit cell of $(C_4MIm)_2[CoBr_4]$ in a view down the *b*-axis. The $CoBr_4$ units are shown in a polyhedral representation.

Table 5. Selected Bond Lengths [Å] for $(C_4MIm)_2[CoBr_4]$

atom	bond length/Å	atom	bond length/Å
Co−*Br*:		**C−*C*:**	
Co1−Br1	2.4070(3)	C2−C3	1.336(4)
Co1−Br2	2.4037(3)		
		C5A−C6A	1.584(5)
		C6A−C7A	1.521(7)
***N*−C:**		C7A−C8A	1.636(7)
N1−C1	1.329(3)		
N1−C3	1.368(3)	C5B−C6B	1.414(5)
N2−C1	1.327(3)	C6B−C7B	1.523(6)
N2−C2	1.374(3)	C7B−C8B	1.283(6)
N1−C4	1.460(3)		
N2−C5/C5A	1.467(3)		

anisotropically. The positions of the hydrogen atoms were calculated on idealized positions and refined using riding models with an isotropic temperature factor 1.5 times as large as that of the attached atom. The butyl group of the imidazolium cation is disordered on two locations (C5A to C8A and C5B to C8B). This situation was refined with the sum of the occupation factors of the two chains being fixed to unity. Finally, the occupation refined to 47.7 % for one chain (and 52.3 %, respectively, for the other). Attempts to obtain a nondisordered model using the lower symmetry space group *C*c failed. Full crystallographic details of this structure determination have been deposited at the Cambridge Crystallographic Data Centre and can be obtained quoting the reference number CCDC-705517.

3. Results and Discussion

3.1. Activity Coefficients at Infinite Dilution. The values of γ_i^∞ of different solutes in $(C_4MIm)_2[CoBr_4]$ obtained at different temperatures are listed in Table 1. Altogether, 108 data points for 19 solutes have been obtained in the temperature range (308 to 413) K. The complete set of data is available in the Supporting Information. The values of γ_i^∞ have been approximated by the linear regression

$$\ln \gamma_i^\infty = a + \frac{b}{T} \tag{4}$$

The coefficients a and b, as well as the values of $\gamma_{i\,(298\ K)}^\infty$ calculated with these coefficients are also given in Table 1. The activity coefficients of the linear *n*-alkanes, *n*-alkenes, alkylbenzenes, and alkanols increase with increasing chain length. Introduction of the double bond in the alkane chain also causes a decrease of γ_i^∞. This indicates a better solubility of molecules with double bonds in the ionic liquid due to their higher polarizability.

Values of γ_i^∞ for benzene and the alkylbenzenes are distinctly lower in comparison with those of the alkanes and alkenes. However, as with alkanes, γ_i^∞ values increase with increasing size of the alkyl group. The activity coefficients of the linear *n*-alkanols slightly increase with increasing chain length.

The value for the partial molar excess enthalpy at infinite dilution $H_i^{E,\infty}$ can be directly obtained from the slope of a straight line derived from eq 5

$$\left(\frac{\partial \ln \gamma_i^\infty}{\partial(1/T)}\right) = \frac{H_i^{E,\infty}}{R} \tag{5}$$

R is the gas constant. The values of $H_i^{E,\infty}$ for the compounds studied are also listed in Table 1. The uncertainties of $H_i^{E,\infty}$ are estimated to be not better than ± 10 % due to the small slope of ln γ_i^∞ versus $1/T$ plots and taking into account the experimental uncertainty of the γ_i^∞ values. This is also confirmed by results of $H_i^{E,\infty}$ for systems where a comparison between the results obtained by eq 5 and direct calorimetric data is possible.[14]

$H_i^{E,\infty}$ for alkanes, alkenes, and alkanols are positive and slightly change with increasing chain length. The introduction of double bonds slightly lowers the positive values of $H_i^{E,\infty}$. Only the value of $H_i^{E,\infty}$ of benzene is negative. For other benzene derivatives, values of $H_i^{E,\infty}$ are positive and only slightly change with increasing chain length.

Values of γ_i^∞ of typical solutes (decane, 1-decene, toluene, and methanol) at 298 K in $(C_4MIm)_2[CoBr_4]$ obtained in this work are compared in Table 2 with results of other (C_4MIm) containing ionic liquids (with general formula $(C_4MIm)[X]$) taken from the literature. No significant differences between paramagnetic and nonparamagnetic ionic liquids are observed.

3.2. Crystal Structure. The single-crystal X-ray structure of the title phase, $(C_4MIm)_2[CoBr_4]$, was determined at 173 K. It crystallizes in the monoclinic space group *C*2/c. The structure is built up from isolated $[CoBr_4]^{2-}$ complex ions and 1-butyl-3-methylimidazolium cations. In the unit cell, the Co atom is located on the Wykhoff site 4e with 2-fold symmetry. The asymmetric unit consists of one-half of the $[CoBr_4]^{2-}$ ion and one imidazolium cation. An Ortep drawing of both the anion and the cation is depicted in Figure 2. Experimental details of the structure determination and the crystallographic data of $(C_4MIm)_2[CoBr_4]$ are presented in Table 3. Table 4 lists the refined atom coordinates and isotropic displacement parameters. The average Co−Br of 2.4054 Å compares well with that found in other compounds with the $[CoBr_4]^{2-}$ ion, for example, in $\{N(CH_3)_4\}_2[CoBr_4]$, which is 2.398 Å.[18] Table 4 lists further bond lengths of the title phase. The Br−Co−Br angles have values in the range of 106.18(1)° to 112.47(2)°. Therefore, the

coordination polyhedron around the Co atom deviates slightly from perfect tetrahedral geometry. As described in the experimental section, the *n*-butyl chain of the cation is disordered on two positions with almost 1:1 occupation. Figure 3 shows the butyl chain disorder of the 1-*n*-butyl-3-methylimidazolium cation. All the distances and angles within the cation are in the expected range. Figure 4 shows the packing of the ions within the unit cell. The shortest nonbonding Co···Co distance is 8.745 Å, a value certainly too long to allow for strong magnetic interaction. A similar distance, although a little smaller, is found in the corresponding chloride, $(C_4MIm)_2[CoCl_4]$.[4] Selected bond lengths [Å] for $(C_4MIm)_2[CoBr_4]$ are given in Table 5.

Acknowledgment

Dedicated to Prof. Dr. Gerhard M. Schneider on the occasion of his 75th birthday.

Supporting Information Available:

Table of critical constants and acentric factors of the solutes and the carrier gas used in calculation of the virial coefficients. This material is available free of charge via the Internet at http://pubs.acs.org.

Literature Cited

(1) Hayashi, S.; Hamaguchi, H. Discovery of a magnetic ionic liquid [bmim]$FeCl_4$. *Chem. Lett.* **2004**, *33*, 1590–1591.

(2) Yoshida, Y.; Saito, G. Influence of structural variations in 1-alkyl-3-methylimidazolium cation and tetrahalogenoferrate(III) anion on the physical properties of the paramagnetic ionic liquids. *J. Mater. Chem.* **2006**, *16*, 1254–1262.

(3) Zhang, Q.-G.; Yang, J.-Z.; Lu, X.-M.; Gui, J.-S.; Huang, M. Studies on an ionic liquid based on $FeCl_3$ and its properties. *Fluid Phase Equilib.* **2004**, *226*, 207–211.

(4) Zhong, C.; Sasaki, T.; Jimbo-Kobayashi, A.; Fujiwara, E.; Kobayashi, A.; Tada, M.; Iwasawa, Y. Syntheses, structures, and properties of a series of metal ion -containing dialkylimidazolium ionic liquids. *Bull. Chem. Soc. Jpn.* **2007**, *80*, 2365–2374.

(5) Kozlova, S. A.; Verevkin, S. P.; Heintz, A.; Peppel, T.; Köckerling, M. Activity Coefficients at Infinite Dilution of Hydrocarbons, Alkylbenzenes, and Alcohols in the Paramagnetic Ionic Liquid 1-Butyl-3-Methyl-Imidazolium Tetrachloridoferrate(III) Using Gas-Liquid Chromatography. *J. Chem. Thermodyn.* **2008**, *40*, 330–333.

(6) Cruickshank, A. J. B.; Windsor, M. L.; Young, C. L. The use of gas-liquid chromatography to determine activity coefficients and second virial coefficients of mixtures. *Proc. R. Soc* **1966**, *A295*, 259–270.

(7) Grant, D. W. *Gas-Liquid Chromatography*; van Nostrand Reinhold Company: London, 1971.

(8) Ruzicka, K.; Majer, V. Simultaneous Treatment of Vapor Pressures and Related Thermal Data Between the Triple and Normal Boiling Temperatures for n-Alkanes C_{5-20}. *J. Phys. Chem. Ref. Data* **1994**, *23*, 1–39.

(9) Steele, W. V.; Chirico, R. D. Thermodynamic Properties of Alkenes (Mono-Olefins Larger Than C_4). *J. Phys. Chem. Ref. Data* **1993**, *22*, 377–430.

(10) Ambrose, D.; Walton, J. Vapour pressures up to their critical temperatures of normal alkanes and 1-alkanols. *Pure Appl. Chem.* **1989**, *61*, 1395–1403.

(11) Heintz, A.; Kulikov, D. V.; Verevkin, S. P. Thermodynamic Properties of Mixtures Containing Ionic Liquids. 1. Activity Coefficients at Infinite Dilution of Alkanes, Alkenes, and Alkylbenzenes in 4-Methyl-N-Butyl-Pyridinium Tetrafluoroborate Using Gas-Liquid Chromatography. *J. Chem. Eng. Data* **2001**, *46*, 1526–1529.

(12) Heintz, A.; Kulikov, D. V.; Verevkin, S. P. Thermodynamic Properties of Mixtures Containing Ionic Liquids. Activity Coefficients at Infinite Dilution of Polar Solvents in 4-Methyl-N-Butyl-Pyridinium Tetrafluoroborate Using Gas-Liquid Chromatography. *J. Chem. Thermodyn.* **2002**, *34*, 1341–1347.

(13) Heintz, A.; Kulikov, D. V.; Verevkin, S. P. Thermodynamic Properties of Mixtures Containing Ionic Liquids. 2. Activity Coefficients at Infinite Dilution of Hydrocarbons and Polar Solutes in 1-Methyl-3-Ethyl-Imidazolium-Bis(trifluoromethyl-sulfonyl) Amide and in 1,2-Dimethyl-3-Ethyl-Imidazolium Bis-(trifluoromethyl-sulfonyl) Amide Using Gas−Liquid Chromatography. *J. Chem. Eng. Data* **2002**, *47*, 894–899.

(14) Heintz, A.; Marczak, W.; Verevkin, S. P. *Ionic Liquids IIIA: Fundamentals, Progress, Challenges, and Opportunities*; Rogers, R. D., Seddon, K., Eds.; ACS Symposium Series 901, American Chemical Society: Washington DC, 2005; Chapter 14, pp 187−206.

(15) Heintz, A.; Casás, L. M.; Nesterov, I. A.; Emel'yanenko, V. N.; Verevkin, S. P. Thermodynamic Properties of Mixtures Containing Ionic Liquids. 5. Activity Coefficients at Infinite Dilution of Hydrocarbons Alcohols, Ester and Aldehydes in 1-Methyl-3-Butyl-Imidazolium Bis(trifluoromethyl-sulfonyl) Imide Using Gas-Liquid Chromatography. *J. Chem. Eng. Data* **2005**, *50*, 1510–1514.

(16) Bruker-Nonius Inc., Apex-2, v. 1.6−8, Saint, v. 6.25a, *SADABS-Software for the CCD detector System*; Madison, WI, USA, 2003.

(17) Sheldrick, G. M. *SHELX97-Programs for crystal structure analysis*, (Release 97−2); University of Göttingen: Göttingen, Germany, 1997.

(18) Nishihata, Y.; Sawada, A.; Kasatani, H.; Terauchi, H. Structure of tetramethylammonium tetrabromocobaltate at room temperature. *Acta Crystallogr. C: Cryst. Struct. Commun.* **1993**, *C49*, 1939–1941.

Received for review November 11, 2008. Accepted February 12, 2009. This work has been supported by the German Science Foundation (DFG) priority program SPP 1191, as well as by the Research Training Group 1213 "New Methods for Sustainability in Catalysis and Technique" (DFG).

JE800846J